

Article

# Recognizing Different Types of Skin Diseases by Using the Efficient Net-B3 Model

Yaarob Younus Al-Badrani<sup>1</sup>, Raid Rafi Omar Al-Nima<sup>2</sup>, Maher Talal Al-Asaady<sup>3\*</sup>

1. Department of Quality Assurance and University Performance, Northern Technical University, Mosul 41001, Iraq
  2. Technical Engineering College of Mosul, Northern Technical University, Mosul 41001, Iraq
  3. Department of Networks and Computer Software, Northern Technical University, Mosul 41001, Iraq
- \* Correspondence: [maher.alasaady@ntu.edu.iq](mailto:maher.alasaady@ntu.edu.iq)

**Abstract:** The skin, as the body's primary defense, faces increased vulnerability to diseases like cancer due to factors such as ozone layer depletion, UV radiation, and infections. Despite advancements in diagnostic tools, accurate and early detection of skin conditions remains a challenge. This study aims to address this gap by proposing a deep learning-based framework using the EfficientNet-B3 model for multi-class classification of eight skin conditions, including malignant and benign types. The approach employs a structured pipeline with data augmentation to enhance the training set, followed by fine-tuning EfficientNet-B3 for improved accuracy. Results show that the optimized model achieves an accuracy and F1-score of 94%, providing a practical and reliable tool for early diagnosis. These findings suggest significant potential for supporting dermatologists, improving patient outcomes, and reducing clinical workload through efficient disease identification.

**Keywords:** Classification, Deep Learning, EfficientNet-B3 Model, Skin Cancer, Transfer Learning

**Citation:** Yaarob Younus Al-Badrani, Raid Rafi Omar Al-Nima, Maher Talal Al-Asaady. Recognizing Different Types of Skin Diseases by Using the Efficient Net-B3 Model. Central Asian Journal of Mathematical Theory and Computer Sciences 2024, 5(4), 465-475.

Received: 19<sup>th</sup> Sept 2024  
Revised: 19<sup>th</sup> Oct 2024  
Accepted: 26<sup>th</sup> Oct 2024  
Published: 2<sup>th</sup> Nov 2024



**Copyright:** © 2024 by the authors. Submitted for open access publication under the terms and conditions of the Creative Commons Attribution (CC BY) license (<https://creativecommons.org/licenses/by/4.0/>)

## 1. Introduction

The human body contains many unusual organs. The skin is one of them. The skin's ectodermal tissue, which can have up to seven layers, shields the internal organs, muscles, bones, and ligaments [1,2]. Skin regulates body temperature and protects against infections. The perception of heat and cold sensations is aided by skin nerves [3]. Human skin comprises an underlying dermis and a stratified cellular epidermis. Figure 1 shows the relationship between the subcutaneous fat layer and the striated muscle layer that separates the dermis from the rest of the body. Human skin cells receive some of the sun's potentially damaging ultraviolet radiation (UV).

Using sunbeds increases the chance of developing skin cancer [4,5]. In the last decade, skin cancer has become the most prevalent form of cancer, with melanoma being the most dangerous and fatal kind. Melanocytes are the cells within which melanoma develops [6, 7]. The World Health Organization (WHO) estimates that 10,000 people every year in the US alone pass away from melanoma, and that the overall death toll will rise by 6.5 percent in 2022. Each year, there are over 100,000 new instances of melanoma found in Europe, while melanoma is found in 15,229 Australians. Melanoma is treatable if found early enough, with survival rates of 96% in the first stage and 5% in the late stage [8, 9].

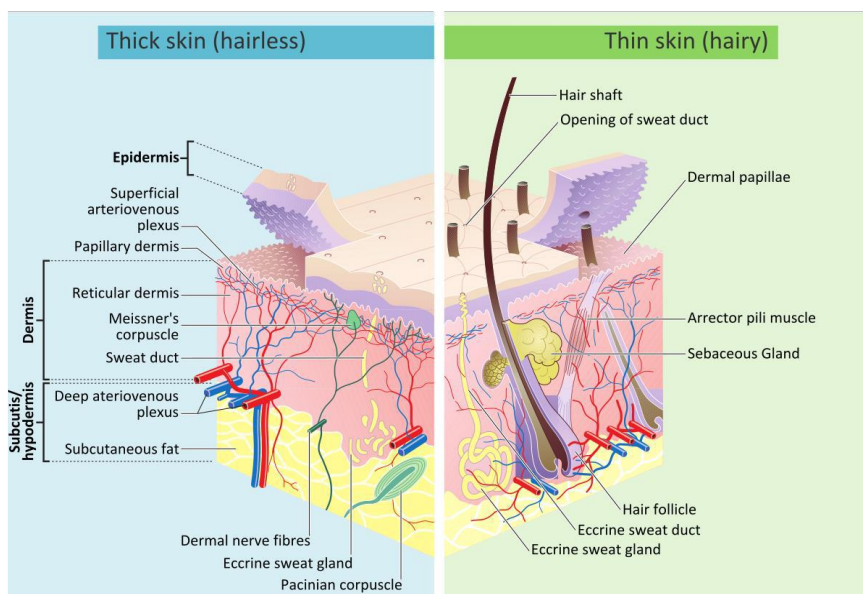


Figure 1. Structure of the inner layers of human skin [8, 9]

The proper diagnosis of skin conditions may be time-consuming and expensive. Medical experts currently have to spend much time physically diagnosing skin illnesses. Our research focuses largely on using big data networks based on deep learning to aid dermatologists and healthcare professionals in the early identification and classification of skin cancer. In addition to assisting medical professionals to save lives with the least amount of work and in the shortest amount of time, we provide appropriate treatment.

Most prior research has focused on classifying individual diseases or a limited number of skin conditions, with relatively few studies addressing the multi-class classification of various skin cancers. This study introduces a deep learning-based algorithm capable of distinguishing between multiple benign and malignant skin lesions, achieving greater accuracy than previous approaches. A key contribution of this work is the use of the EfficientNet-B3 model, specifically selected for its ability to classify eight distinct types of skin diseases, as illustrated in Figure 2.



Figure 2. Examples of the eight different types of diseases caused by skin lesions.

This paper is organized as follows: Section 1 provides the introduction, Section 2 reviews previous studies, Section 3 illustrates the methodology, Section 4 discusses results and Section 5 reveals the conclusion.

### Literature Review

In 2019, Sriwong et al. suggested a deep learning model of a Convolutional Neural Network for the categorization of skin diseases (CNN). Both picture data and prior information about the patients were used in the modeling procedure to improve classification performance. AlexNet model, SVM model for feature extraction data, and SVM model for feature extraction of image and patient were investigated. The findings of the experiment indicated that, of the three models, the SVM model for feature extraction of the patient's picture displayed the greatest performance [10].

In 2019, Andersen proposed using deep learning techniques to distinguish between malignant melanoma and benign tumors. The study employed Convolutional Neural Networks (CNNs), including a custom 6-layer CNN. A balanced subset of the ISIC dataset was specifically used to differentiate melanomas from benign lesions [11].

In 2020, Rezaoana et al. proposed an automated technique for skin cancer classification, focusing on identifying nine different types of skin cancer. The study evaluated the performance and effectiveness of a deep CNN model. The primary objective was to develop a model capable of accurately detecting skin cancer and distinguishing between multiple classes [12].

In 2020, Mohan et al. provided a computer-aided tool for skin cancer screening. This was the main topic of this research. Dermoscopic images served as the Computer-Assisted Diagnostic (CAD) input data. The aim of the study was to estimate the prevalence of skin cancer in humans using CNN features and a pre-trained network of Residual Networks-50 [13].

In 2021, Arshad et al. proposed a framework for classifying multiple types of skin lesions. The process involved three augmentation techniques: rotating images by 90°, flipping them horizontally, and flipping them vertically. Next, the deep learning models were fine-tuned, with ResNet-50 and ResNet-101 being employed and their layers adjusted. Finally, transfer learning was applied to train the refined models on the augmented dataset. The findings indicated that the data augmentation significantly enhanced the classification accuracy [14].

In 2021, Datta et al. suggested a method of investigating the effectiveness of soft-attention in deep learning architectures. Soft-attention's primary goal was to emphasize crucial details while downplaying distracting ones. Comparisons were considered for the capabilities and efficiency of the soft-attention-based deep learning architecture in image analysis by categorizing skin lesions using the Visual Geometry Group (VGG), Residual Networks (ResNet), Inception ResNet version 2, and Dense Network (DenseNet) architectures with and without the soft-attention mechanism [15].

In 2022, Khan et al. introduced a Deep Generative Adversarial Network (DGAN) for multi-class skin cancer classification. The framework incorporated two CNN models, built using ResNet50 and VGG16 architectures, to assess the effectiveness of the GAN. The study applied traditional augmentation techniques, such as rotation, flipping, and scaling, to enhance the training datasets. However, the performance of the models was significantly impacted by the limited availability of labeled training data [16].

In 2022, Bechelli and Delhommelle evaluated how well traditional machine learning and deep learning models performed when analyzing dermoscopic pictures of skin lesions. Additionally, the research showed that deep learning models typically outperform traditional machine learning models, particularly when CNN models were used to represent the fine-grained variability of dermoscopic pictures [17].

In 2022, Dimililer and Sekeroglu utilized a CNN with different training configurations to classify malignant, non-cancerous, and other types of skin lesions using a dataset collected through mobile phones. The design incorporated a specific number of epochs, and a transfer learning approach was applied to enhance the model's performance [18].

It is challenging for researchers to classify many types of skin lesions because of their striking similarities. The vast majority of recent research that categorizes skin cancer using deep learning techniques, including CNN, attempted to divide skin cancer into two groups: benign and malignant. In our work, we attempt to categorize eight forms of skin cancers despite the challenge of such a task.

## 2. Materials and Methods

### Proposed EfficientNet-B3 model

The Efficient Network (EfficientNet) family of architectures was created to increase the accuracy (model performance) and efficiency of CNNs via scalability (model parameters) [19]. A compound scaling technique is suggested that scales width, depth, and resolution in an equal manner using a specified set of coefficients. This method was used to develop the Efficient Network version B0 (EfficientNet-B0). Additionally, versions B1 to B7 of EfficientNet can be constructed by scaling the baseline model (EfficientNet-B0) using the same compound scaling method. This approach adjusts the network's depth, width, and resolution proportionally. As a result, [19, 20] present the performance of these CNN architectures across eight different scales.

Efficient Network version B7 (EfficientNet-B7) contains 66 million parameters and requires an input image size of 600×600 pixels, compared to Efficient Network version B3 (EfficientNet-B3) which contains 10.7 million parameters and requires an input image size of 300×300 pixels. By altering the network depth and breadth, CNN may capture properties that are richer and more complex [21]. The top three levels were replaced with additional layers for our use case, which included classifying skin cancer into eight categories. The applied EfficientNet-B3 model exhibited significant overfitting due to its top three layers. Consequently, these layers were removed, and additional dense, batch normalization, and dropout layers were incorporated. As a result, the new top three layers now consist of batch normalization, dropout, and global average pooling. Figure 3 depicts the upgraded version of EfficientNet-B3.

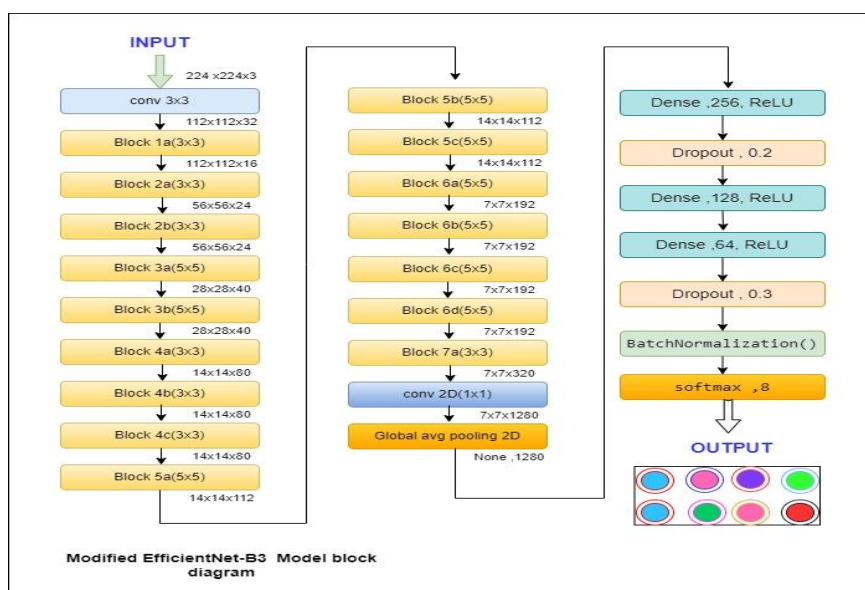


Figure 3. Model Diagram of an improved version of EfficientNet-B3 that is employed in this study.

### Data normalization

In this research, data normalization is taken into account. Normalization is the process of transforming data into a common range [22]. Pre-processing is essential to avoid the dominance of large numerical values over smaller ones [23]. Z-score normalization, min-max normalization, and neural network normalization are examples of existing data normalizing approaches. Z-score normalization is done using the formula below:

$$z_i = \frac{x_i - \mu}{\sigma} \quad (1)$$

where  $z_i$  is an output value,  $x_i$  is an input value,  $i = 1, 2, \dots, n$ ,  $n$  is a number of considered input values,  $\mu$  is a mean value and  $\sigma$  is a variance value.

$$\mu = \frac{1}{n} \sum_{i=1}^n x_i \quad (2)$$

$$\sigma = \sqrt{\frac{1}{n-1} \sum_{i=1}^n (x_i - \mu)^2} \quad (3)$$

The normalization process maps the input data to be in the range between 0 and 1.

### Data augmentation

The amount of training data that a network corresponds to and its capacity have a strong positive correlation [24]. In this work, data augmentation is used to raise the number of skin cancer picture inputs to 52,794. This growth may enhance network capability and effectiveness (see Table 1).

Table 1. Augmentation operations for images of considered skin cancer types.

Augmentation Method	Parameter Value	Action
Horizontal Shift (Range)	0.2	Randomly shifts images horizontally (as a fraction of total width).
Rotation Range	90°	Rotates images randomly within a 0° to 180° range.
Vertical Flip	True	Randomly flips images vertically.
Zoom Level	0.1	Randomly zooms into the image.
Shear Range	0.15	Specifies the cropping range for the image.
Horizontal Flip	True	Randomly flips images horizontally.
Vertical Shift (Range)	0.2	Randomly shifts images vertically (as a fraction of total height).

### Performance evaluation metrics

To evaluate the performance of our classification method, the following metrics are used:

#### Confusion matrix

A confusion matrix is a table that considers counting the number of instances for a dataset that falls into a specific category. That is, a category of True Positive (TP), False Negative (FN), False Positive (FP) and True Negative (TN). A general recognition confusion matrix is shown in Table 2 [25].

Table 2. General recognition confusion matrix.

		Predicted Class	
		Positive	Negative
Actual Class	True	TP	FN
	False	FP	TN

### Accuracy

The proportion of accurately predicted classes to all utilized images is represented by the word "Accuracy". The following equation illustrates the accuracy (*Accuracy*) computation equation:

$$Accuracy = \frac{TP+TN}{TP+TN+FP+FN} \times 100\% \quad (4)$$

where *Accuracy* is the calculated accuracy, *TP* is the TP, *TN* is the TN, *FP* is the FP and *FN* is the FN [26].

### Precision

Precision measures the percentage of how many images that the model is properly classified as belonging to a positive class divided by the number of images which are correctly classified. The calculated precision (*Precision*) equation can be expressed as follows [26]:

$$Precision = \frac{TP}{TP+FP} \times 100\% \quad (5)$$

where *Precision* is the computed precision.

### Recall

The recall is the percentage of all correctly classed positive samples to the correctly classed positive samples and incorrectly classed negative samples. It can be represented as [26]:

$$Recall = \frac{TP}{TP+FN} \times 100\% \quad (6)$$

where *Recall* is the calculated recall.

### F1-score

Measuring F1-score, commonly known as the F measure, is used in statistical analysis for binary classification. For a full assessment of a model's performance in the context of a multiclass classification task, the F1-score (*F1 – score*) is computed over all classes using the following expression [27].

$$F1 - score = 2 \times \frac{Precision \times Recall}{Precision + Recall} \times 100\% \quad (7)$$

where *F1 – score* is the computed F1-score.

## 3. Results and Discussion

In this work, two melanoma databases were used, and many images of diverse skin tumours were acquired. The two groups were combined and mixed to raise their total number of pictures to 7,542 photos in order to maximize the number of datasets pertaining to benign and malignant melanoma and enhance the performance of the EfficientNet-B3.

The International Skin Imaging Collaboration (ISIC) archive repository has the first dataset, it has been provided in [28]. This dataset has 5,629 images for five different types of skin cancers. The second dataset is also from the ISIC archive; it has been provided in [29]. This dataset has 1,913 images for malignant and benign cancers. Each image is high-resolution in Joint Photographic Experts Group (JPEG) format and of size 450×600 pixels.

Multiple kinds of skin cancer are depicted in the training and test datasets. Some examples of these types of cancers are basal cell carcinoma (BCC), squamous cell

carcinoma (SCC), melanoma (MEL), actinic keratosis (AK), seborrheic keratosis (SK), vascular lesions (VASC), and melanocytic nevi (MV). Table 3 shows the distribution of photos for each form of cancer in the datasets.

Table 3. Number of images for each type of cancer in the utilized datasets.

Dataset	Number of Images for Each Type of Skin Cancer							
	AK	BCC	DF	MV	MEL	SK	SCC	VASC
The first dataset [28]	1125 Images	1127 Images	-	1125 Images	1126 Images	1126 Images	-	-
Second dataset [29]	130 Images	197 Images	246 Images		438 Images	80 Images	569 Images	253 Images
The total number of images				7,542 images				

### Results and discussions of training and validation

First of all, the EfficientNet-B3 base architecture layers are modified in this study, where more dense, batch normalization and dropout layers are added. The ReLU activation function is also considered for dense layers and completely connected layers. All images in the datasets are partitioned as 70%, 20%, and 10% for training, validation and testing.

Here are the settings for EfficientNet-B3's training parameters: Adam, an Adaptive Moment Estimation technique, is used to improve the model with a learning rate (LR) of 0.001. If the accuracy does not improve after three consecutive epochs, a callback function is used to lower the LR by a factor of 0.5. There is a 32-batch limit during training, and the maximum number of epochs is 35. To further improve the model's performance, fine-tuning is also implemented.

Figure 4(a) displays the accuracy curves for both training and validation. On top of that, figure 4(b) displays the loss curves for instruction and verification. They prove that training and validating EfficientNet-B3 were successful in terms of performance.

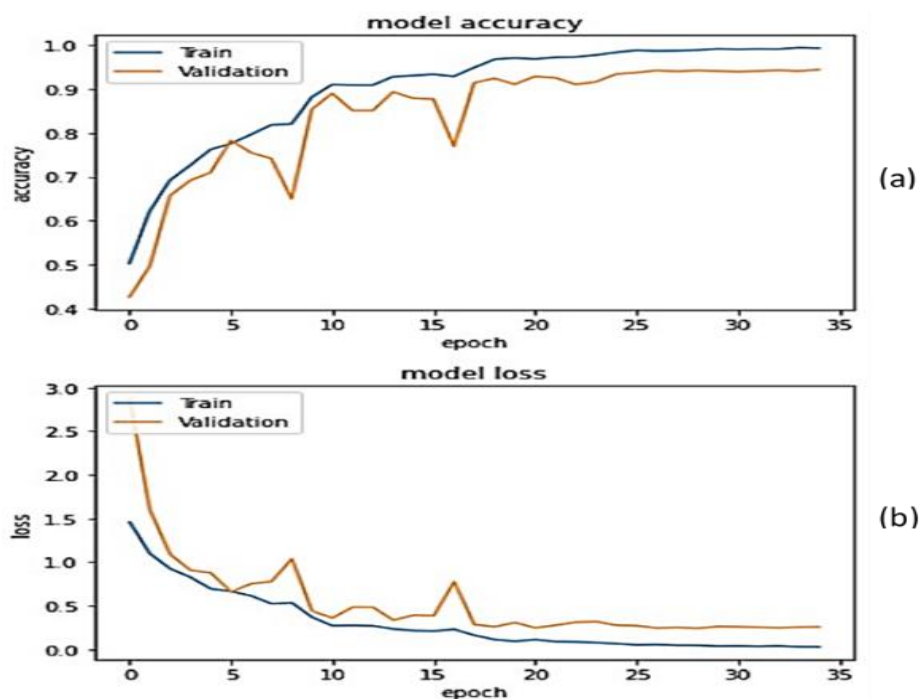


Figure 4. The training and validation curves for accuracy and loss, respectively.

Given that the training accuracy grows, and the training loss curve gradually decreases as the number of iterations increases, the model has got successful training. Also, there is no overfitting risk during training as there are close differences between the training and validation curves.

### Results and discussions of testing

The efficacy of the proposed EfficientNet-B3 model was assessed by examining the outcomes on the residual test samples post-training. The fine-tuned model attained an accuracy of 93.75%, demonstrating its successful learning from the training process and its proficiency in properly identifying the majority of the test data. The findings indicate that the EfficientNet-B3 model can accurately classify eight distinct kinds of skin cancer.

### Confusion matrix and classification report

The model was evaluated using a test set of 762 randomly selected images. As shown in Figure 5, the confusion matrix reveals high values along the diagonal for all eight skin cancer classes, indicating that the model performs well in accurately categorizing each type. These results confirm the model's effectiveness in classifying the eight skin cancer types based on the provided testing data.

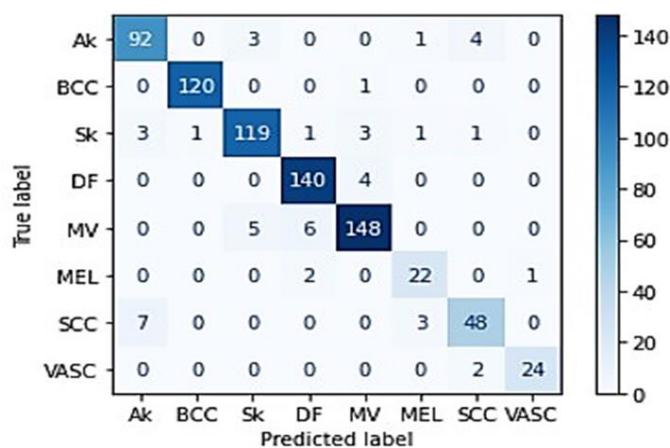


Figure 5. Confusion Matrix for the suggested EfficientNet-B3 Model.

The performances of the updated EfficientNet-B3 model are evaluated by using the accuracy, precision, recall, and f1-score. The macro averages of all eight classes of skin cancer types have reached 92% for each metric. Furthermore, the weighted averages of the considered skin cancer types have reported 94% for each metric. The best values of precision, recall and f1-score can be found for the BCC. Table 4 shows obtained values of the employed metrics for all classes. It shows that our model has successfully completed its.

Table 4. Obtained values of the employed metrics for each and all classes.

Class(s)	Precision	Recall	F1-score
AK	90%	92%	91%
BCC	99%	99%	99%
SK	94%	92%	93%
DF	94%	97%	96%
MV	95%	93%	94%
MEL	81%	88%	85%
SCC	87%	83%	85%
VASC	96%	92%	94%
Macro average	92%	92%	92%
Weighted average	94%	94%	94%
Overall accuracy	94%		

### Comparisons

For comparisons, other deep learning networks or models are simulated and used. The outcomes of the applied comparisons are displayed in Table 5. Table 5 presents a comparison of the testing accuracies achieved by various deep learning networks, highlighting differences in their performance when classifying different types of skin cancer. The results indicate that the proposed EfficientNet-B3 model outperforms the others, achieving the highest accuracy, demonstrating its suitability for this multi-class skin cancer classification task. Networks' accuracies after fine-tuning were 77.02%, 80.70, 80.39%, 81.25%, 79.45% and 91.7% for the VGG-16 [28], VGG-19 [30], AlexNet [10], CNN [11], CNN [12] and ResNet-50 [14], respectively. They were all lower than the accuracy of the proposed EfficientNet-B3 model. The work in this paper can also be utilized to develop other skin studies such as [31], [32] and [33].

Table 5. Comparisons of different deep learning models for classifying diverse populations of skin cancer.

Deep Learning Model	Pre-processing	Accuracy after fine-tuning	Dataset
VGG-16 [28]	Augmentation	77.02 %	ISIC
VGG-19 [30]	Augmentation	80.70 %	ISIC
AlexNet [10]	---	80.39%	ISIC
CNN [11]	Contrast enhancement	81.25%	ISIC
CNN [12]	Image processing	79.45 %	ISIC
ResNet-50 [14]	Augmentation	91.7%	HAM10000
Proposed EfficientNet-B3 model	Augmentation	94%	ISIC

### 4. Conclusion

Skin cancer is a serious and potentially life-threatening condition, with survival rates significantly improving through early detection. The risk of developing skin cancer can be heightened by factors such as viral and fungal infections, as well as prolonged exposure to ultraviolet radiation. In this context, deep learning techniques play a crucial role in enhancing the accuracy and efficiency of skin cancer diagnosis and classification. This study focused on examining the use of one of the deep learning networks to categorize skin cancer images. The proposed contribution model of the updated EfficientNet-B3 model was adopted. The main processing stages were considered. Firstly, collecting skin

cancer images, where 7,542 images of malignant and benign oncological diseases (up to 8 skin cancer types) were collected. After that, augmentation operations were employed. The images used were allocated into three groups: 70% for training, 20% for validation, and 10% for testing. The fine-tuned model demonstrated excellent performance in multi-classifying skin lesions. Evaluations revealed that the proposed EfficientNet-B3 model, enhanced with data augmentation, achieved up to 94% accuracy across the two combined datasets. This study offers valuable support for dermatologists and researchers in classifying eight distinct types of skin cancer.

## REFERENCES

- [1] M. Vestita, P. Tedeschi, and D. Bonamonte, "Anatomy and Physiology of the Skin," in *Textbook of Plastic and Reconstructive Surgery: Basic Principles and New Perspectives*, M. Maruccia and G. Giudice, Eds. Cham: Springer International Publishing, 2022, pp. 3–13.
- [2] M. Harahap, A. M. Husein, S. C. Kwok, V. Wizley, J. Leonardi, D. K. Ong, D. Ginting, and B. A. Silitonga, "Skin Cancer Classification Using EfficientNet Architecture," *Bulletin of Electrical Engineering and Informatics*, vol. 13, no. 4, pp. 2716–2728, 2024.
- [3] Cleveland Clinic, "Skin: Layers, Structure, and Function," [Online]. Available: <https://my.clevelandclinic.org/health/articles/10978-skin>. Accessed Dec. 28, 2022.
- [4] M. Uhlén, L. Fagerberg, B. M. Hallström, et al., "Proteomics. Tissue-Based Map of the Human Proteome," *Science*, vol. 347, no. 6220, p. 1260419, Jan. 2015, doi: 10.1126/science.1260419.
- [5] C. R. Prasad, G. Bilveni, B. Priyanka, C. Susmitha, D. Abhinay, and S. Kollem, "Skin Cancer Prediction Using Modified EfficientNet-B3 with Deep Transfer Learning," in *2024 IEEE International Conference for Women in Innovation, Technology & Entrepreneurship (ICWITE)*, 2024, pp. 519–523.
- [6] M. Dildar, S. Akram, M. Irfan, H. U. Khan, M. Ramzan, A. R. Mahmood, S. A. Alsaieri, A. H. M. Saeed, M. O. Alraddadi, and M. H. Mahnashi, "Skin Cancer Detection: A Review Using Deep Learning Techniques," *International Journal of Environmental Research and Public Health*, vol. 18, no. 10, p. 5479, 2021. [Online]. Available: [https://mdpi-res.com/d\\_attachment/ijerph/ijerph-18-05479/article\\_deploy/ijerph-18-05479.pdf](https://mdpi-res.com/d_attachment/ijerph/ijerph-18-05479/article_deploy/ijerph-18-05479.pdf).
- [7] M. Sakl, C. Essid, B. B. Salah, and H. Sakli, "DL Methods for Skin Lesions Automated Diagnosis in Smartphone Images," in *2023 International Wireless Communications and Mobile Computing (IWCMC)*, 2023, pp. 1142–1147.
- [8] A. Naeem, T. Anees, M. Fiza, R. A. Naqvi, and S.-W. Lee, "SCDNet: A Deep Learning-Based Framework for the Multiclassification of Skin Cancer Using Dermoscopy Images," *Sensors*, vol. 22, no. 15, p. 5652, 2022. [Online]. Available: [https://mdpi-res.com/d\\_attachment/sensors/sensors-22-05652/article\\_deploy/sensors-22-05652-v2.pdf](https://mdpi-res.com/d_attachment/sensors/sensors-22-05652/article_deploy/sensors-22-05652-v2.pdf).
- [9] V. Venugopal, N. I. Raj, M. K. Nath, and N. Stephen, "A Deep Neural Network Using Modified EfficientNet for Skin Cancer Detection in Dermoscopic Images," *Decision Analytics Journal*, p. 100278, 2023.
- [10] K. Sriwong, S. Bunrit, K. Kerdprasop, and N. Kerdprasop, "Dermatological Classification Using Deep Learning of Skin Image and Patient Background Knowledge," *International Journal of Machine Learning and Computing*, vol. 9, no. 6, pp. 862–867, 2019.
- [11] C. A. R. Andersen, "Melanoma Classification in Low Resolution Dermoscopy Images Using Deep Learning," M.S. thesis, The University of Bergen, Norway, 2019.
- [12] N. Rezaoana, M. S. Hossain, and K. Andersson, "Detection and Classification of Skin Cancer by Using a Parallel CNN Model," in *2020 IEEE International Women in Engineering (WIE) Conference on Electrical and Computer Engineering (WIECON-ECE)*, 2020, pp. 380–386.
- [13] M. Mohan, J. Ram, and K. Gopalakrishnan, "Melanoma Skin Cancer Classification Using Deep Learning Convolutional Neural Network," *Medico-Legal Update*, vol. 20, pp. 351–355, 2020.
- [14] M. Arshad, M. A. Khan, U. Tariq, et al., "A Computer-Aided Diagnosis System Using Deep Learning for Multiclass Skin Lesion Classification," *Computational Intelligence and Neuroscience*, vol. 2021, 2021.

- [15] S. K. Datta, M. A. Shaikh, S. N. Srihari, and M. Gao, "Soft Attention Improves Skin Cancer Classification Performance," in *Interpretability of Machine Intelligence in Medical Image Computing, and Topological Data Analysis and Its Applications for Medical Data*, Springer, 2021, pp. 13–23.
- [16] M. Heenaye-Mamode Khan, N. Gooda Sahib-Kaudeer, M. Dayalen, et al., "Multi-Class Skin Problem Classification Using Deep Generative Adversarial Network (DGAN)," *Computational Intelligence and Neuroscience*, vol. 2022, 2022.
- [17] S. Bechelli and J. Delhommelle, "Machine Learning and Deep Learning Algorithms for Skin Cancer Classification from Dermoscopic Images," *Bioengineering*, vol. 9, no. 3, p. 97, 2022. [Online]. Available: [https://mdpi-res.com/d\\_attachment/bioengineering/bioengineering-09-00097/article\\_deploy/bioengineering-09-00097-v2.pdf](https://mdpi-res.com/d_attachment/bioengineering/bioengineering-09-00097/article_deploy/bioengineering-09-00097-v2.pdf).
- [18] K. Dimililer and B. Sekeroglu, "Skin Lesion Classification Using CNN-Based Transfer Learning Model," *Gazi University Journal of Science*, vol. 35, no. 4, pp. 1512–1519, 2022.
- [19] M. Tan and Q. Le, "EfficientNet: Rethinking Model Scaling for Convolutional Neural Networks," in *International Conference on Machine Learning*, 2019, pp. 6105–6114.
- [20] A. Rafay and W. Hussain, "EfficientSkinDis: An EfficientNet-Based Classification Model for a Large Manually Curated Dataset of 31 Skin Diseases," *Biomedical Signal Processing and Control*, vol. 85, p. 104869, 2023.
- [21] N. T. Dinitra, I. Wijayanto, F. Akhyar, A. S. Safitri, and R. S. Firdhaust, "Enhancing Skin Cancer Classification Using EfficientNet-Based Architectures," in *2024 International Conference on Data Science and Its Applications (ICoDSA)*, 2024, pp. 415–420.
- [22] M. T. Alasaady, "Comparative Study Between Object-Oriented Software Engineering and Agent-Oriented Software Engineering," *International Journal of Software Engineering*, vol. 7, no. 5, pp. 28–34, 2017.
- [23] M. T. Alasaady, M. G. Saeed, and K. H. Faraj, "Evaluation and Comparison Framework for Data Modeling Languages," in *Proc. 2019 2nd International Conference on Electrical, Communication, Computer, Power and Control Engineering (ICECCPCE)*, Feb. 2019, pp. 68–73.
- [24] D. Vishal, M. V. Manikandaprabhu, B. Vishnuvardhan, and S. Yuvaraj, "A Study on Machine Learning Models for Segmentation and Classification of Skin Diseases," in *AIP Conference Proceedings*, 2024, vol. 3035, no. 1, AIP Publishing.
- [25] G. Shobha and S. Rangaswamy, "Machine Learning," in *Handbook of Statistics*, vol. 38, Elsevier, 2018.
- [26] A. Bassel, A. B. Abdulkareem, Z. A. A. Alyasseri, N. S. Sani, and H. J. Mohammed, "Automatic Malignant and Benign Skin Cancer Classification Using a Hybrid Deep Learning Approach," *Diagnostics*, vol. 12, no. 10, p. 2472, 2022. [Online]. Available: [https://mdpi-res.com/d\\_attachment/diagnostics/diagnostics-12-02472/article\\_deploy/diagnostics-12-02472-v2.pdf](https://mdpi-res.com/d_attachment/diagnostics/diagnostics-12-02472/article_deploy/diagnostics-12-02472-v2.pdf).
- [27] K. Ali, Z. A. Shaikh, A. A. Khan, and A. A. Laghari, "Multiclass Skin Cancer Classification Using EfficientNets—A First Step Towards Preventing Skin Cancer," *Neuroscience Informatics*, vol. 2, no. 4, p. 100034, 2022.
- [28] A. W. Khan, "Skin Cancer Dataset," [Online]. Available: <https://www.kaggle.com/datasets/abdulwadoodkhan199/skin-cancer-dataset>.
- [29] J. Ahuja, "Skin Cancer Detection Using CNN," [Online]. Available: <https://www.kaggle.com/datasets/jaiahuja/skin-cancer-detection>.
- [30] A. W. Khan, "Skin Cancer Dataset-VGG19," [Online]. Available: <https://www.kaggle.com/code/abdulwadoodkhan199/skin-cancer-using-transfer-learning-vgg19>.
- [31] R. R. O. Al-Nima, M. K. Jarjes, A. W. Kasim, and S. S. M. Sheet, "Human Identification Using Local Binary Patterns for Finger Outer Knuckle," in *2020 IEEE 8th Conference on Systems, Process and Control (ICSPC)*, 2020, pp. 7–12.
- [32] R. R. Al-Nima, "Design a Biometric Identification System Based on the Fusion of Hand Geometry and Backhand Patterns," *Iraqi Journal of Statistical Sciences*, vol. 10, no. 1, pp. 169–180, 2010.
- [33] R. R. Al-Nima, "Human Authentication With Earprint for Secure Telephone System," *Iraqi Journal of Computers, Communications, Control and Systems Engineering IJCCCE*, vol. 12, no. 2, pp. 47–56, 2012.